



# Science in a cup of coffee: A structural study of a trigonelline aqueous solution

Michael Di Gioacchino, Maria Antonietta Ricci, Fabio Bruni \*

Dipartimento di Scienze, Università degli Studi di Roma Tre, Via della Vasca Navale 84, 00146 Roma, Italy

## ARTICLE INFO

### Keywords:

Trigonelline aqueous solution  
Neutron diffraction  
EPSR  
Zundel and Eigen cations  
Coffee

## ABSTRACT

Bioactive trigonelline is one of the important components of coffee, contributing to its characteristic undue bitterness. In this report we looked at the structure of an aqueous solution of trigonelline by means of Neutron Diffraction with Isotopic Substitution (NDIS). This experimental approach has been coupled with a Monte Carlo simulation to get an atom-level description of the solution. The rationale behind the present study is to investigate the solvent-solute and the solute-solute interactions; these have implications relevant also to other bioactive molecules and, in addition, can provide basic information on the extraction efficiency and on the solubility of important molecules in coffee. Results indicate a limited short-ranged involvement of the solute trigonelline with the water solvent and a not negligible clustering of trigonelline molecules. The investigated solution contains both positively charged and zwitterionic trigonelline, along with  $\text{Cl}^-$  and  $\text{H}^+$ , with this latter ion involved in hydronium ion formation. Here it is found that the observed structures are compatible with a Zundel-like cation, thus contributing to the still on-going debate on the presence of either Zundel or Eigen complexes in acidic solution. The role of a Zundel-like cation, along with its interaction with the chloride ion, might be related to the extraction and solubility of important molecules in coffee, in order to define the best water composition resulting in the best coffee.

## 1. Introduction

For sheer sensory enjoyment, few everyday experiences can compete with a good cup of coffee. The alluring aroma of steaming hot coffee just brewed from freshly roasted beans can drag sleepers from bed and pedestrians into cafés. But underlying this seemingly commonplace beverage is a profound chemical complexity that demands detailed knowledge of its composition [1]. Caffeine, trigonelline and nicotinic acid (vitamin  $\text{B}_3$ ) are three important bioactive components of coffee [2–4]. In particular, trigonelline belongs to major components of coffee, where it is present in amounts similar to those of caffeine [5–7]. Trigonelline, a methyl betaine of nicotinic acid, is found in various plants and seeds [8,9], it crystallizes as monohydrate, and its structure has been determined by X-ray diffraction [10,11]. Trigonelline (Fig. 1, panel A) is an alkaloid with chemical formula  $\text{C}_7\text{H}_8\text{ClNO}_2$  (see Materials and Methods section), is highly water soluble, and it is the most substantial element that contributes to undue bitterness in coffee. It has been reported to have hypoglycemic, hypolipidemic, sedative, antimigraine, antibacterial, antiviral, and anti-tumor effects, and to improve memory retention and inhibit platelet aggregation [12].

Despite its high solubility and abundance in aqueous solvent (i.e. coffee), trigonelline-water interactions are largely unknown, and whether or not this molecule interacts preferably with water through hydrogen bonding, or binds to other trigonelline molecules through electrostatic interactions, is still an open issue for this bioactive molecule. Detailed knowledge on this issue might have implications also for vitamin  $\text{B}_3$  interactions with water, still largely unknown [13], as this vitamin is produced by demethylation of trigonelline during coffee bean roasting. The rationale of the present study is to investigate trigonelline-water interactions at the atomistic level with a neutron diffraction experiment augmented with a computer simulation. In particular, we want to look and compare solute-water and solute-solute interactions. This information will likely shed light on solvent accessibility and hydration of specific trigonelline sites at atomistic level, and on the possible formation of trigonelline chains being mediated or not by water molecules. In this context and regarding solute-solvent interactions, in a previous and recent study, we looked at the hydration of the carboxylate group of different biomolecules, including trigonelline [14]. The main result of this latter report was to identify the key role

\* Corresponding author.

E-mail address: [fabio.bruni@uniroma3.it](mailto:fabio.bruni@uniroma3.it) (F. Bruni).

<https://doi.org/10.1016/j.molliq.2024.123972>

Received 9 October 2023; Received in revised form 15 December 2023; Accepted 3 January 2024

Available online 9 January 2024

0167-7322/© 2024 The Author(s). Published by Elsevier B.V. This is an open access article under the CC BY license (<http://creativecommons.org/licenses/by/4.0/>).

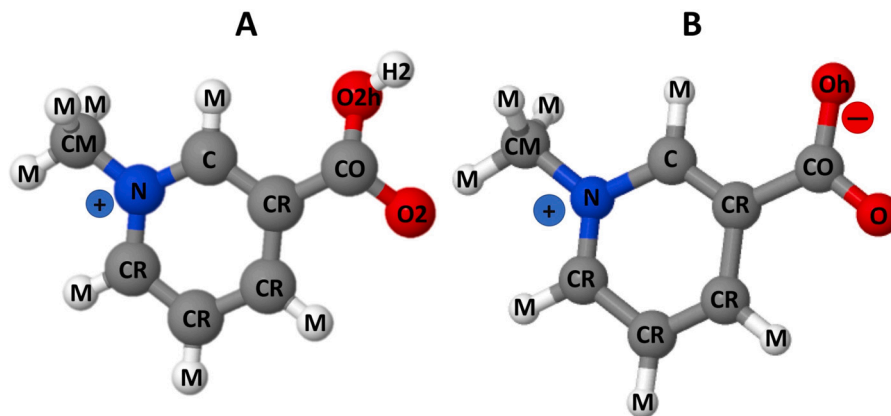


**Fig. 1.** Stick and ball structure of the trigonelline molecule. Carbon atoms are shown in gray, hydrogen atoms in white, oxygen atoms in red, and the nitrogen in blue. Different atom labels indicate different potential parameters used in the EPSR simulation, as listed in Table 1. **Panel A** Structure of hydrochloride trigonelline. **Panel B** Structure of zwitterionic trigonelline. In panel A and B the dissociated  $\text{Cl}^-$  ion not shown.

played by the carboxylate group with respect to solute-solvent interactions.

Regarding the coffee making process, the outcome of the present study could provide a basic framework essential to carry on future studies on the extraction efficiency of trigonelline from ground coffee as a function of the ions present in water. This latter sentence is based on the well known, but still poorly understood, Hofmeister series, whose predictions indicate that calcium and magnesium ions in the water used to brew coffee should enhance the solubility of important molecules in coffee, trigonelline included. This subject is still in its infancy as very little is known about the best water composition, namely identity and relative amount of dissolved ions, resulting in the best coffee [15,16].

## 2. Materials and methods

The aim of the present study is to investigate trigonelline-water interactions with a Neutron Diffraction experiment with Isotopic Substitution (NDIS) experiment combined with an Empirical Potential Structure Refinement (EPSR) simulation. Neutron diffraction experiments have been performed using the SANDALS neutron diffractometer, installed at the ISIS Facility (U.K.) [17–19]. To fully exploit the advantages of isotopic substitution, a set of isotopically labeled samples were prepared as follows. Trigonelline hydrochloride was purchased from Sigma-Aldrich and used without further purification. Aqueous solutions were prepared by dissolving the solute in water to obtain solutions at a concentration of 1.11 M, corresponding to approximately 1 solute (trigonelline) molecule in 50 water molecules, resulting in a measured pH equal to 1.03. It should be noted that if dissolved in water, hydrochloride trigonelline carboxyl group (-COOH) can be deprotonated, ending up as carboxylate group (-COO<sup>-</sup>). This resulting zwitterionic structure of trigonelline is shown in Fig. 1, panel B. Starting from the water solubility limit of trigonelline, that is 1000 g/L, we can estimate the minimum number of water molecules required to dissolve each trigonelline molecule. Given trigonelline hydrochloride molecular weight, that is 173.60 g/mol, the minimum number of water molecules is about 10 per each solute molecule, that is clearly smaller than the ratio (1 solute to 50 solvent molecules) investigated in the present study. The concentration of the investigated samples is much higher compared to trigonelline concentration in a standard cup of coffee (about 20 mM) but adequate to have, on one side, enough water molecules to fully hydrate the solute and, on the other side, a measurable scattered intensity not due to water only. As discussed above, 10 water molecules are enough to fully hydrate each trigonelline solute, extra water molecules do not play any role in determining the balance between solute-solvent and solvent-solvent interactions, and, as such, the results of the present experiment should be not dependent on sample concentration. To obtain isotopically substituted trigonelline aqueous solutions, trigonelline

was dissolved in water and also in a fully deuterated water solvent. In addition, an equimolar mixture of these two solutions was prepared. In the following we will refer to these three samples as T-H<sub>2</sub>O, T-D<sub>2</sub>O, and T-HDO, respectively. The substitution of H atoms with D atoms is crucial to enhance scattering contrast of the investigated solutions, as it will be made clear below. NDIS experiments were performed at  $T = 298$  K, and data have been collected also for the empty instrument, empty container and niobium-vanadium standard, in order to normalize the data for all investigated samples to an absolute scale of differential cross-section. Diffraction data have been processed by using the “GudrunN” suite of programs [20], which performs corrections for multiple scattering, absorption, inelasticity effects, and scattering from the sample container, and samples themselves. “GudrunN” also verifies that the measured scattered intensity is consistent with sample density and composition.

The outputs of “GudrunN” are the total neutron-weighted interference differential cross sections (IDCS) defined as

$$F(Q) = \sum_{\alpha} \sum_{\beta \geq \alpha} w_{\alpha\beta} [S_{\alpha\beta}(Q) - 1] \quad (1)$$

where  $\alpha$  and  $\beta$  label the atomic sites,  $Q$  is the magnitude of the change in the momentum vector by the scattered neutrons, defined as  $Q = 4\pi \sin\theta / \lambda$  where  $2\theta$  represents the scattering angle and  $\lambda$  the wavelength of scattered radiation. The functions

$$S_{\alpha\beta}(Q) = 4\pi\rho \int_0^{\infty} r^2 (g_{\alpha\beta}(r) - 1) \frac{\sin Qr}{Qr} dr, \quad (2)$$

called partial structure factor (PSF), are the Fourier transforms of the individual site-site radial distribution function  $g_{\alpha\beta}(r)$ , and  $\rho$  is the atomic number density of the investigated solution. The individual PSFs are weighted in Eq. (1) by  $w_{\alpha\beta} = c_{\alpha}c_{\beta}b_{\alpha}b_{\beta}(2 - \delta_{\alpha\beta})$ , where  $c_{\alpha}$  and  $c_{\beta}$  are the concentrations of the  $\alpha$  and  $\beta$  nuclei, and  $b_{\alpha}$  and  $b_{\beta}$  are their scattering lengths [21], respectively.

Thus, each experimental IDCS is a linear combination of many PSFs, and in order to extract from the available experimental data information on the individual site-site radial distribution functions, direct Fourier transform of the IDCS or of combinations of the experimental data is of limited usefulness. In liquids with a small number of distinct atoms, like H<sub>2</sub>O, by measuring an array of different isotopically labeled samples, it is possible to directly extract all of the pair correlation functions from the experiment, giving a direct assessment of the hydrogen bonding present in the measured liquid. However, in more complex samples, like those investigated in the present report, it is not possible to isotopically label every atom site; for this reason, we employ a simulation-assisted procedure that has been developed in the past two decades in order to

**Table 1**

Reference potential parameters used in the EPSR simulation for the investigated aqueous solution of trigonelline. Atoms are labeled according to Fig. 1. The simulation box contains 55 positively charged trigonelline molecules, 5 zwitterionic trigonelline molecules, 60  $\text{Cl}^-$ , 5  $\text{H}^+$  ions, and 3000 water molecules. The EPSR simulation allows rotations of the carboxylate group. The distinction between the two oxygens in the zwitterionic configuration, namely Oh and O listed below, is made possible given this EPSR feature.

Atom label	$\epsilon$ (kJ/mol)	$\sigma$ (Å)	$q$ (e)
O2h	0.71128	3.00	-0.58
O2	0.87864	2.96	-0.50
H2	0	0	0.45
Oh	0.71128	3.00	-0.58
O	0.87864	2.96	-0.50
CO	0.43932	3.75	0.55
CR	0.31400	3.80	-0.146
C	0.31400	3.80	-0.146
CM	0.08370	4.55	0.36
$\text{N}^+$	0.83700	4.55	0.90
M	0	0	0
$\text{Cl}^-$	0.419	4.38	-0.90
$\text{H}^+$	0.075	0	0.90
Hw	0	0	0.4238
Ow	0.65	3.166	-0.8476

convert IDCS data to real space, with extraction of the whole set of radial distribution functions. This is called EPSR [18,19] and is similar in principle to the methods routinely used in crystallography, which attempt to systematically refine a structural model to give best overall agreement with the diffraction data. This method is currently the most informative available for refining these structures in the liquid state, and it has been so far successfully employed to investigate the interaction of small molecules with water, see for instance [22–35]. EPSR is based on a Monte Carlo routine, which refines an interaction potential and a real space structural model of the sample against the experimental data, starting from a seed potential model and a random distribution of molecules in the simulation box. Provided that the simulation box has the same composition and density as those of the real sample, EPSR outputs a reliable structural model of the investigated solution that could be used to obtain information otherwise not accessible with an experimental study alone. Importantly, the seed potential model, usually a Lennard-Jones potential plus fractional charges, must be suited to represent the real sample. In the present case, the interaction model for trigonelline has been adapted from [36]. The simple point charge/extended (SPC/E) model [37] has been used to describe water interactions. After equilibrating on the seeding potential for over about  $10^3$  iterations, we started the potential refinement loop. During this phase of the data analysis, the algorithm iteratively adds a numerical correction to the analytical seeding potential that guides the configuration toward an improved agreement with the data. Once the fit cannot improve further, the production run can start, with statistics accumulated over at least  $10^4$  configurations. Further details on the EPSR procedure can be found in ref. [18,19]. In the present instance, the EPSR simulation box is built with the same density and composition as the real samples. In particular, the number of fully dissociated trigonelline molecules has been obtained according to the measured pH value of the solution (*i.e.* 1.03), as this value dictates the number of  $\text{H}^+$  ions released in solution by the trigonelline carboxyl group. Given the concentration of the aqueous trigonelline solution along with its measured pH, the resulting EPSR simulation box contains 55 trigonelline molecules ( $\text{C}_7\text{H}_8\text{NO}_2$ , Fig. 1, panel A), 5 zwitterionic trigonelline molecules ( $\text{C}_7\text{H}_7\text{NO}_2$ , Fig. 1, panel B), 60  $\text{Cl}^-$  and 5  $\text{H}^+$  ions, along with 3000 water molecules. The size of the cubic simulation box is 47.44 Å, yielding a solution density equal to 0.095 atoms/Å<sup>3</sup>. This latter density value is consistent with the value reported by “GudrunN” routine, as indicated above. Table 1 lists the potential parameters for the EPSR routine.

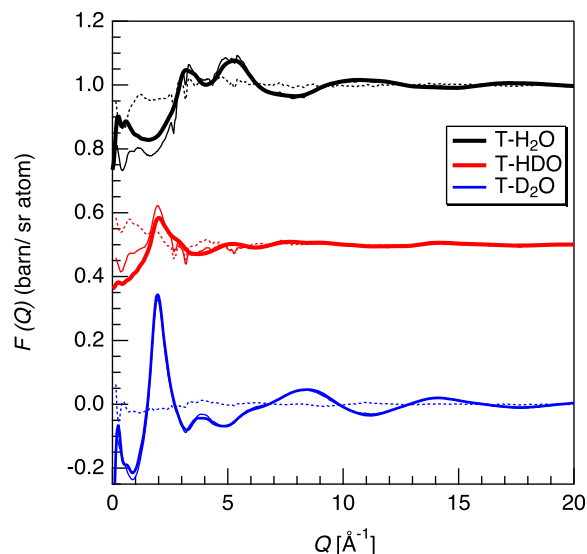


**Fig. 2.** Interference differential cross section as a function of  $Q$  for the three samples investigated, namely T- $\text{H}_2\text{O}$ , T- $\text{D}_2\text{O}$ , and T-HDO. Thick solid lines are the result of the EPSR procedure, thin solid lines are the original data, dashed lines the residues. The overall quality of the fit is good, as shown by flat residues for  $Q \geq 2 \text{ \AA}^{-1}$ . Notice the presence of misfits at very low  $Q$  with no relevance on the assessment of the local structure of the solution, as they will result in small unfitted features at very large distances in real space. Data have been vertically shifted for clarity.

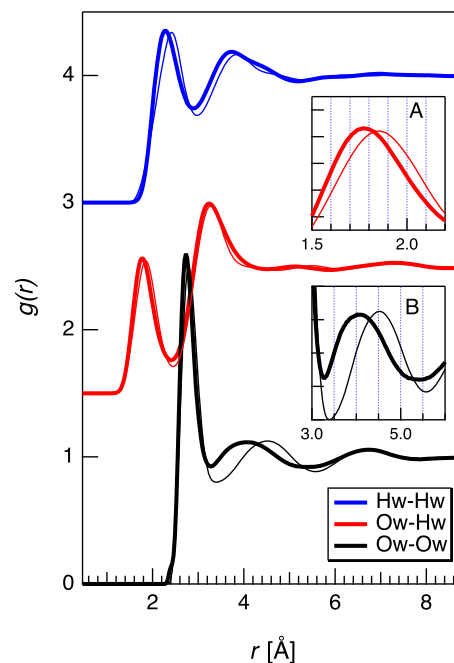


**Fig. 3.** Radial distribution functions of water atoms. Thick solid lines are the radial distribution functions for water as a solvent, while thin solid lines represent the same functions for pure water (data collected at  $T = 300 \text{ K}$ ). Notice the reduction of the hydrogen bond length (zoomed in the insert A), along with the large shift to shorter distance of the second peak of the  $g_{\text{OwOw}}(r)$  (zoomed in the insert B), suggesting a perturbation of the water structure. Data have been vertically shifted for clarity.

Of particular interest in the framework of the present study, are quantities that could be obtained by EPSR, namely the full set of radial distribution functions,  $g_{\alpha\beta}(r)$ , the running coordination number,  $n_{\alpha\beta}(r)$ , and the Spatial Density Functions (SDF) [38]. The running coordination

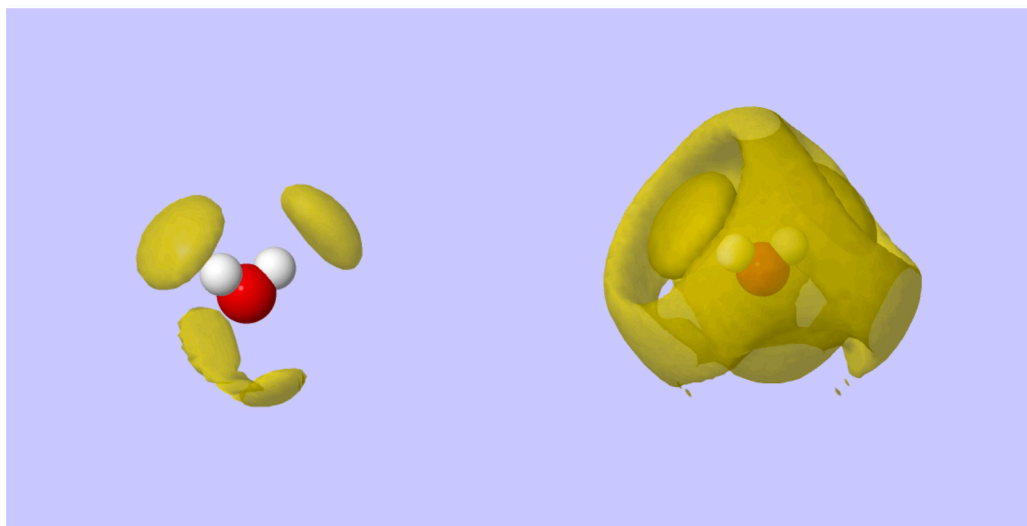


**Fig. 4.** Spatial Density Function (SDF) of the first and second shell of solvent water molecules around a water oxygen atom in the origin of the reference frame. These SDFs represent the probability, above a given threshold value of 35% and within a set distance, of finding a water molecule, however oriented. The left panel in Fig. 4 shows as yellow clouds the first shell obtained within the range (0.0–3.3) Å, while the right panel shows both the first and second shell, obtained within the range (0.0–5.5) Å from the water oxygen atom in the origin. These distance ranges are taken from the first and second minima of the  $g_{OwOw}(r)$ , see Fig. 3.

number represents the number of  $\beta$  sites within a distance  $r$  from site  $\alpha$ , defined by:

$$n_{\alpha\beta}(r) = 4\pi\rho c_{\beta} \int r^2 g_{\alpha\beta}(r) dr \quad (3)$$

where  $r$  is the distance between atomic site  $\alpha$ , at the origin of the reference frame, and  $\beta$ . The SDF functions combine the radial and angular distribution functions, rendering a 3D-cloud reconstruction of the neighbor shells of a specific molecule around a chosen atom placed in the origin of a reference frame.

### 3. Results and discussion

Fig. 2 shows the results of the EPSR analysis of the collected data. We note the overall good agreement between the measured data and the EPSR fits. The residuals, also shown in Fig. 2, indicate the absence of features not properly fitted by the EPSR simulation, beside some misfits at  $Q < 0.75 \text{ \AA}^{-1}$  due to the difficulty associated with a complete subtraction of the large recoil between hydrogen atoms and neutrons. It should be noted that these misfits have no effects on the assessment of the hydration structure of the solute, given their very low  $Q$  position, resulting in small features at very large distances in the real space. Regarding the relative weight of the solute trigonelline on the total interference cross section, this turns out to be about 8% of the total measured cross section. However, EPSR code provides the R-factor, or discrepancy index, which measures the disagreement between the observed structure factor amplitudes and the calculated amplitudes as resulting from the model. This turns out to be about 0.03%. The difference between these two reference values suggests that solute-solvent and solute-solute interactions are well observable and larger than the fit residues. Regarding the values of the intermolecular distances and coordination numbers that will be discussed in the following, the associated uncertainties are therefore limited to the second decimal place.

Given that EPSR provides a reliable model of the real investigated aqueous trigonelline solution, we can now look at the simulation box to calculate quantities otherwise not accessible with an experimental approach only. The first of these quantities, is the hydrogen bonded structure of water as a solvent. Fig. 3 shows the site-site radial distribution functions of water atoms, namely Ow and Hw. In particular, the largest difference with pure water (data included in Fig. 3 as thin solid lines are taken from reference [39]) is shown by the  $g_{OwOw}(r)$ . This

radial distribution function shows a second peak shifted to a shorter distance (peak centered around  $r = 4.0 \text{ \AA}$ ) compared to pure water. Such inward shifts are usually taken as the signature of a modification of the tetrahedral network of pure water, and have been interpreted in terms of an equivalent pressure, that is the external pressure that should be applied to pure water to reproduce the observed peak shift [40,41]. On these grounds, we can estimate, given the measure of the second peak shift, a value for the equivalent pressure close to 300 MPa [42]. It should be noted, however, that the analogy between external pressure applied to neat water and presence of solutes in solutions resulting in similar inward shifts of the second peak of the  $g_{OwOw}(r)$  has been recently questioned by a careful DFT approach [43]. This latter work does not support this analogy, yet this conclusion has been reached without no direct comparison between the experimental [40,41] and the simulated radial distribution functions of water as a solvent. It is fair to state that the issue related to the analogy between pressure and solute concentration is not settled yet. Other notable differences between neat and water as a solvent, albeit less evident, can be found both in the  $g_{HwHw}(r)$  and in the  $g_{OwHw}(r)$ . In the first case, we observe an increased orientational disorder of water hydrogens, visible as a shallower separation between first and second peak, along with a shift to shorter distances of all peaks. The Ow-Hw correlation indicates a quite strong intermolecular H-bond at  $r = 1.8 \text{ \AA}$ , to be compared to the same bond in pure water at  $r = 1.9 \text{ \AA}$ .

These results can be also better seen with a 3D representation of the spatial arrangement of water molecules around a central water molecule. Fig. 4 shows the Spatial Density Function (SDF) of the first and second shell of solvent water molecules around a water oxygen atom in the origin of the reference frame. This function represents the probability, above a given threshold and within a set distance, of finding a water molecule however oriented. The left panel in Fig. 4 shows as yellow clouds the first shell, while the right panel shows both the first and second shell. A clear modification of the tetrahedral network of water as a solvent, compared to its bulk configuration [44], can be appreciated as a collapse of the second shell on the first one, as already evidenced by the second peak of the  $g_{OwOw}(r)$ . Perturbation to the water tetrahedral network is, for the investigated solution, due to the combined effect of the trigonelline molecule, of its zwitterionic counterpart, and to the presence of  $\text{H}^+$  and  $\text{Cl}^-$  ions in solution. This latter contribution will be discussed at the end of this section.



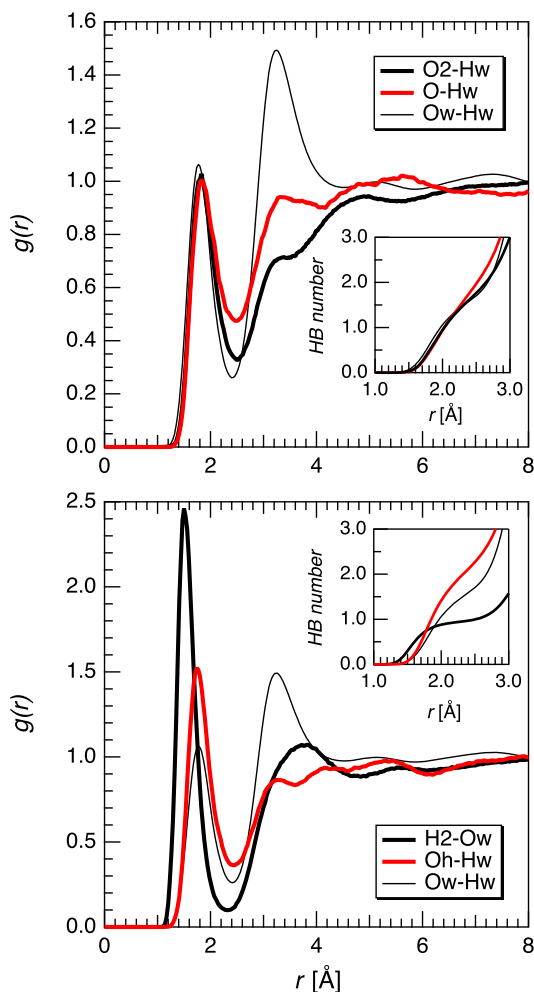


**Fig. 5. Top panel.** Radial distribution functions of oxygen sites (O2 and O) with water hydrogens (Hw), shown as thick solid lines. Thin solid line represents the  $g_{OwHw}(r)$  for water as a solvent, shown also in Fig. 3. The first peak, around  $r = 1.8 \text{ \AA}$  is the signature of an hydrogen bond. The number of these bonds as a function of  $r$  is shown in the insert. Hydrogen bond lengths and number are listed in Table 2. **Bottom panel.** Radial distribution functions of carboxyl H2 and carboxylate Oh with water oxygens (Ow) and water hydrogens (Hw), respectively. The first peak, around  $r = 1.5 \text{ \AA}$  for the  $g_{H2Ow}(r)$ , and  $r = 1.7 \text{ \AA}$  for the  $g_{OhHw}(r)$  is the signature of an hydrogen bond. The number of these bonds as a function of  $r$  is shown in the insert. Hydrogen bond lengths and number are listed in Table 2.

With respect to the hydrogen bond (HB) made by water with specific trigonelline sites, such as the hydrogen and oxygen of the carboxyl group (Fig. 1, panel A), and the two oxygens of the carboxylate group (Fig. 1, panel B), these can be obtained by looking at Fig. 5. This figure shows the relevant radial distribution functions, namely  $g_{O2Hw}(r)$  and  $g_{OHw}(r)$  in the top panel of Fig. 5 and the  $g_{H2Ow}(r)$  and  $g_{OhHw}(r)$  in the bottom panel of Fig. 5, to be compared with  $g_{OwHw}$ . Oxygen sites of both the carboxyl and carboxylate group of trigonelline are involved in hydrogen bonding with water hydrogens, as evidenced by the first peak of the radial distribution functions located at  $1.8 \text{ \AA}$ . The number of such bonds is given by the insert of Fig. 5 (top panel), reading the value corresponding to the position of the first minimum of the radial distribution functions. As shown in Fig. 5 (top panel), the HB length made by these two oxygen sites is similar to that made by water oxygen in water as a solvent, albeit their number is slightly larger for the oxygen of the carboxyl group (O2), compared to the oxygen of the carboxylate group (O) and Ow (see Table 2). The number of hydrogen bonds made by water as a solvent is smaller than its bulk water value (i.e. around 1.8, see

**Table 2**

Hydrogen bond (HB) lengths and numbers. HBs listed are made by Ow, Oh, and O with Hw. HB numbers are calculated at the first minimum of the corresponding radial distribution function (see Fig. 5 and inserts). The number of HBs made with water oxygens by H2 should be compared to the number of HBs made by Hw with Ow.

Atomic site	HB length	HB number
Ow	$1.8 \text{ \AA}$	1.6
Hw	$1.8 \text{ \AA}$	0.8
O2	$1.8 \text{ \AA}$	1.8
O	$1.8 \text{ \AA}$	2.0
H2	$1.5 \text{ \AA}$	1.0
Oh	$1.7 \text{ \AA}$	2.2

for instance [39,44]). It should be noted that while the Ow-Hw correlation indicates a clear shell structure extending up to  $5 \text{ \AA}$  from any given water oxygen in the origin of the reference frame, the correlation between trigonelline oxygen sites (both of the carboxyl and carboxylate groups) with water hydrogens suggests a more uniform distribution of water molecules around the solute, beyond the first hydration shell (see Fig. 5, top panel). Notably, the correlation between O2 and Hw shows a larger excluded volume effect [45], namely the effect due to the volume of the solute where water molecules are not allowed, visible as a sloping increase of the  $g_{O2Hw}(r)$ , compared to the same effect shown by the O-Hw correlation. With respect to the perturbation of the water structure, the latter observation suggests a larger effect due to the positively charged trigonelline, compared to its zwitterionic counterpart.

Quite a different picture emerges by looking at the hydrogen bonds made by water with the hydrogen (H2) site of trigonelline carboxyl group and by the oxygen site (Oh) of the carboxylate group (Fig. 5, bottom panel). In both instances, the HB is shorter, thus stronger, and their number is sensibly larger compared to the number of HBs made by water as a solvent (see insert in Fig. 5, bottom panel, and Table 2). The correlation between H2 and Ow shows a better defined first peak and first minimum compared to solvent water, and partially recovers a clear shell structure, compared to the correlation between the oxygen sites (O2, O, and Oh) with Hw. Interestingly, while the first peak of the  $g_{H2Ow}(r)$  is shifted to a shorter distance, the second peak is shifted to a larger distance compared to the correlation between Ow and Hw (Fig. 5, bottom panel). This constraint on the water oxygens might be consistent with the shift to a shorter distance of the second peak of the  $g_{OwHw}(r)$  discussed above (see Fig. 3), thus providing additional support to the equivalent pressure scenario.

Not surprisingly methyl hydrogens (labeled as M in Fig. 1) are not involved in hydrogen bonds with water, as shown in Fig. 6, and as found in [30,32]. Somewhat more surprisingly is that the positively charged nitrogen site of trigonelline makes bonds neither with the solvent, possibly due to the steric hindrance of the nearby  $-\text{CH}_3$  site (see Fig. 1 and 6), nor with negative  $\text{Cl}^-$  ion (see below and Fig. 10). Notably, both M and  $\text{N}^+$  sites correlate with water oxygens, as shown also by the rapidly increasing coordination number (Fig. 6, right axis). In particular, there is one water oxygen first neighbor of each M site within a distance of  $2.9 \text{ \AA}$ , and one water oxygen first neighbor of the nitrogen site within a distance of  $3.5 \text{ \AA}$ . The large values of the coordination numbers with increasing distance from the solute (Fig. 6, right axis) provide support for a uniform and homogeneous presence of water molecules around each trigonelline molecule, albeit not in the solute first hydration shell.

At this stage it would be interesting to check if the limited short-ranged involvement of the solute trigonelline with the water solvent (summing up values in Table 2, and considering a weighted average of the HBs made by the positively charged and zwitterionic trigonelline molecules, there are about 4 water molecules hydrogen bonded to each trigonelline) leaves room for solute-solute interactions. The limited number of zwitterionic trigonelline molecules in the simulation box does not allow an easy observation of clustering involving zwitterionic molecules, and as a consequence only the possible occurrence

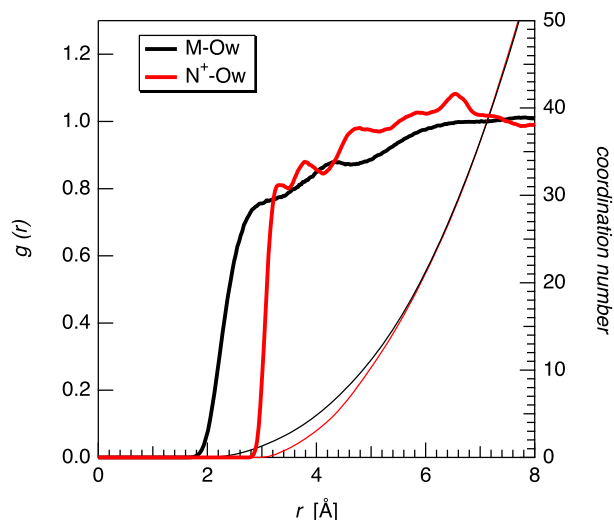


**Fig. 6.** Left axis. Radial distribution function of methyl hydrogens (M) with water oxygen (Ow), black thick solid line, and the same function for positively charged nitrogen ( $N^+$ ) with water oxygen (Ow), red thick solid line. For trigonelline atoms position and label refer to Fig. 1. The right axis shows (thin solid lines with the same color coding) the running coordination number of the M-Ow and  $N^+$ -Ow interactions.

of clustering involving positively charged molecules will be discussed in the following. Fig. 7 (panel A, left axis) shows the intermolecular radial distribution functions of the O2 site of the carboxyl group with the nitrogen site and with the methyl hydrogens (see Fig. 1 for atom labels). The relatively large peak located around 3.3 Å suggests a non negligible correlation between O2 and the nitrogen site, with a coordination number of about 0.65 at a distance of 7.0 Å (see Fig. 7, panel A, right axis). In other words, on average in the simulation box each trigonelline molecule has another trigonelline molecule within a distance of about 7.0 Å with a probability of about 65%. The interaction between trigonelline molecules results in small chains, and it is not water mediated, as it can be seen from a snapshot of the simulation box (see Fig. 7, panel B and C). The correlation of the O2 site with the methyl hydrogens (see Fig. 7, panel A) is broader and with no distinct peaks, with a rapidly increasing coordination number (see Fig. 7, panel A). This is to be expected, given the null charge on methyl hydrogens and their large number.

On the grounds of all of the above observations, it is reasonable to state that trigonelline as a solute exerts a sensible electrostrictive effect on water, altering its tetrahedral structure, is not largely involved in hydrogen bonding with the solvent, and a non negligible fraction of the trigonelline molecules in solution is involved in small clusters.

Trigonelline is not the only solute in the aqueous solution investigated, given the presence of ions, namely  $H^+$  and  $Cl^-$ . In the EPSR simulation box representing the investigated sample, there are 5  $H^+$  ions released in the solution by the Oh site of the carboxyl group (see Fig. 1, panel B), along with 60  $Cl^-$  dissociated from the trigonelline  $N^+$  site. Starting with the proton, its inclusion in the water solvent results in a characteristic double structure of the first peak of the  $g_{H^+Ow}(r)$ , as shown in Fig. 8. This double structure closely resembles what has been seen in *ab initio* simulations and also experimentally, and it has been interpreted as the signature of an asymmetric Zundel complex ( $H_5O_2^+$ ), or alternatively, as distorted Eigen complex ( $H_9O_4^+$ ), see for instance ref. [46] and references therein. The running coordination number (Fig. 8, right axes), confirms this observation, as it shows that every  $H^+$  ion has exactly one water molecule at a distance of 1.1 Å, making a hydronium ion,  $H_3O^+$ . A second water molecule is found at the slightly farther distance of 1.3 Å, thus supporting the presence of a Zundel-like structure, with the  $H^+$  ion bridging between two water molecules, resulting in a Ow-Ow distance of about 2.4 Å. Notably, this latter finding of the EPSR

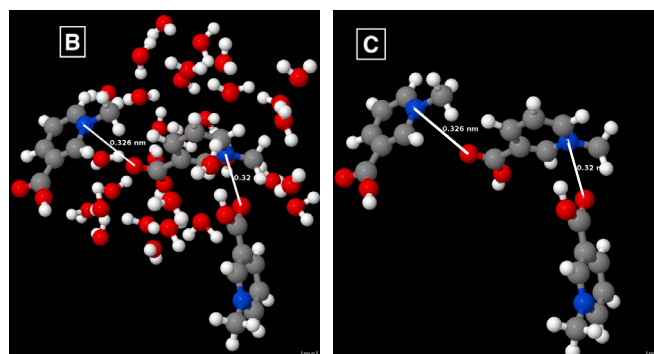
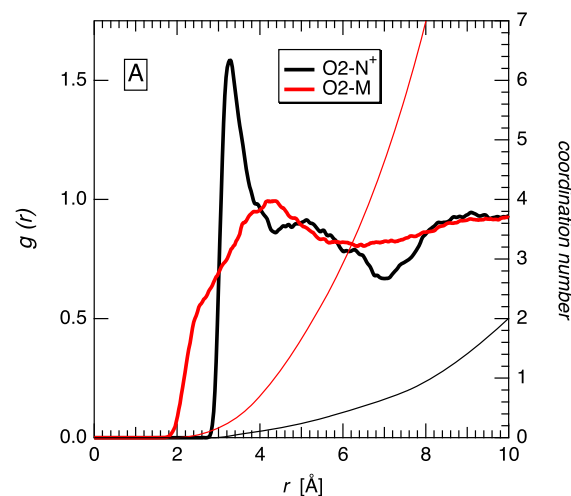


**Fig. 7.** Panel A, left axis. Radial distribution function of carboxyl oxygen site (O2) of a trigonelline molecule, with either nitrogen ( $N^+$ ) or methyl hydrogens (M) of a different trigonelline molecule. The right axis shows (thin solid lines with the same color coding) the running coordination number of the O2- $N^+$  and O2-M interactions. Panel B. A snapshot of the EPSR simulation box showing water molecules around a trigonelline cluster. Distances between  $N^+$  (blue color) and O2 site (red color) of a three-membered cluster are indicated with white lines. Panel C. Same as panel B, but with water molecules removed from the snapshot, showing that the interaction between trigonelline molecules in the cluster is not water mediated.

analysis of the trigonelline-water solution here reported, is obtained without any requirements for the simulation to adopt specific Eigen or Zundel geometries, as it was done in ref. [46], thus providing new information on the hydration of the  $H^+$  ion in solution. Inspection of the radial distribution function of the  $H^+$ -Hw correlation, shows a distinct peak at  $r = 1.9$  Å, followed by a broad peak at about  $r = 4.0$  Å (Fig. 8), consistent with previous data (see Fig. 4 of ref. [46]). The running coordination number indicates that each  $H^+$  ion has 4.0 water hydrogens within a distance of 2.5 Å (right axes of Fig. 8), that again is consistent with the presence of a Zundel-like complex in solution, see for instance [47,48] and references therein.

Regarding the chloride ion environment, Fig. 9 shows the radial distribution function of the  $Cl^-$ -Hw and of the  $Cl^-$ -Ow correlations, along with the respective running coordination numbers (Fig. 9, right axes). As expected, the hydration shell of the chloride ion is made up by about 6.6 water molecules within a distance of 4 Å [49]. The  $Cl^-$ -Hw and the  $Cl^-$ -Ow first neighbor distances are 2.28 Å and 3.21 Å, respectively, in good agreement with the findings of ref. [51], describing the chloride/ $H_2O$  first hydration shell for HCl solution in the concentration range 6.0 *m*–16.1 *m* (molality, *m*, is given as *mol* per kg of solvent). However, we have no evidence for a reduced  $Cl^-$ -Ow bond length for the chloride/ $H_3O^+$  structure, observed as a peak at 2.98 Å [51], possibly due to the lower  $Cl^-$  concentration in our investigated solution (1.1 *m*). As discussed above, our results support the presence of Zundel-

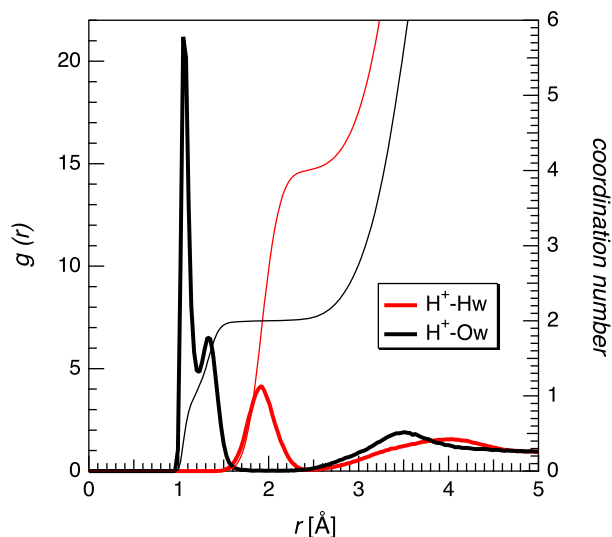


**Fig. 8.** Left axis. Radial distribution functions of the excess proton ( $H^+$ ), dissociated from the carboxyl group of trigonelline, with water atoms Ow and Hw (thick solid lines). The right axis shows (thin solid lines with the same color coding) the running coordination number of the  $H^+$ -Ow and  $H^+$ -Hw interactions.

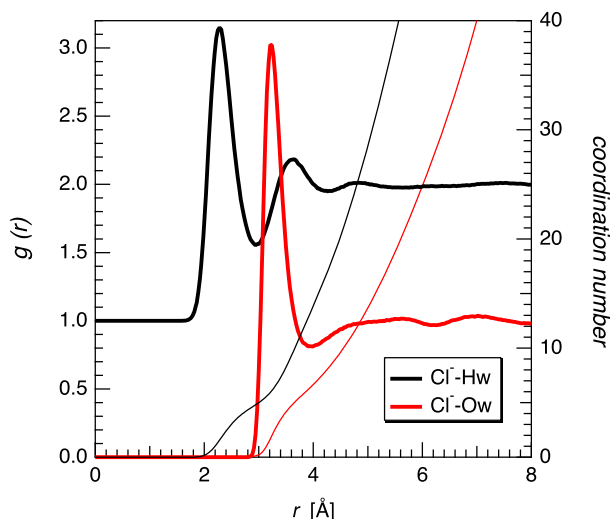


**Fig. 9.** Left axis. Radial distribution functions of the chloride ion ( $Cl^-$ ), dissociated from the nitrogen site of trigonelline, with water atoms Hw and Ow (thick solid lines). The  $g_{Cl^-Ow}(r)$  has been vertically shifted for clarity. The right axis shows (thin solid lines with the same color coding) the running coordination number of the  $Cl^-$ -Hw and  $Cl^-$ -Ow interactions.

like ions in the investigated solution. Further support can be obtained by looking at the  $Cl^-$ - $H^+$  radial distribution function, shown in Fig. 10, indicating a first peak at about 3.6 Å. This latter distance is not compatible with a direct contact between the chloride ion with the  $H^+$  site of an hydronium ion, as required for a Eigen complex, and is instead compatible with the presence of a bridging proton between  $Cl^-$  and Ow in a Zundel-like complex [51]. Clearly, the small number of  $H^+$  in the investigated simulation box prevents to reach a firmer conclusion.

Fig. 10 shows also the  $g_{Cl^-N^+}(r)$  with a first peak located at about 4.0 Å, and with a coordination number (Fig. 10, right axis) that reaches a value of 1.0 at about 8.0 Å. This finding suggests the absence of direct contacts between the chloride ion and the trigonelline molecule. Given the running coordination number of the chloride ion with either water atoms (Hw, Ow) or with the  $H^+$  ion, it is reasonable to conclude that the environment of chloride is made up by water molecules, with only

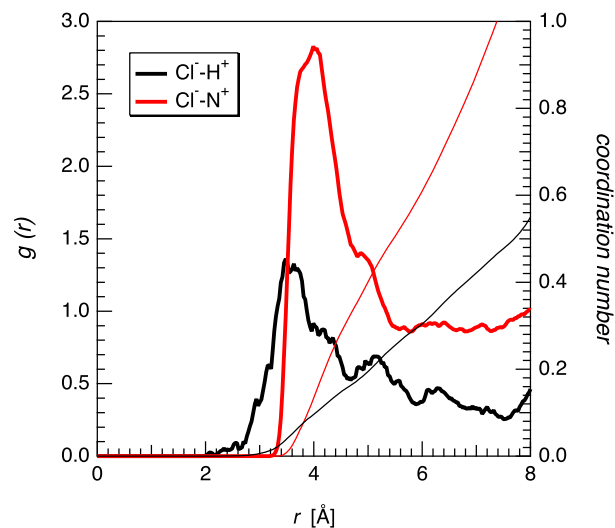


**Fig. 10.** Left axis. Radial distribution function of the chloride ion ( $Cl^-$ ), dissociated from the nitrogen site ( $N^+$ ) of trigonelline (red thick solid line), and with the excess proton in solution,  $H^+$  (black thick solid line). The right axis shows (thin solid lines with the same color coding) the running coordination number of the  $Cl^-$ - $H^+$  and  $Cl^-$ - $N^+$  interactions.

a relatively small number of contacts with Zundel-like complexes (see Fig. 9, 10).

This issue brings us back to the Hofmeister series, and on the role of  $Cl^-$  on the water structure and, in particular, in the extraction procedure of the solute trigonelline during coffee preparation. As already found in the literature [49,50,52–56], the presence of  $Cl^-$  in water does not sensibly alter water tetrahedral network, and its direct interaction with the  $N^+$ -site of trigonelline is negligible (see Fig. 10, right axes). According to the findings of the present report, the largest effect on the structure of water is brought by the presence of solute trigonelline, both as single isolated molecules and as small clusters, and that this effect could be interpreted in terms of an equivalent pressure (see Fig. 3). On the other hand, one cannot exclude at this stage that other solutes added to a trigonelline-water solution might perturb the structure of water and, as a consequence, enhance the extraction outcome to a larger extent. As stated in the Introduction, the issue related to the extraction and solubility of important molecules in coffee, is still in its infancy as very little is known about the best water composition, resulting in the best coffee.

#### 4. Conclusions

In the present report we have investigated with neutron diffraction experiments the structure of an aqueous solution of trigonelline with a concentration equal to 1.1 M and a measured pH equal to 1.03. Data have been used as constraints for a EPSR simulation; the result is a simulation box that is a realistic replica of the real sample, thus allowing a detailed description of the solvent-solvent, solute-solute and solvent-solute interactions. Trigonelline perturbs to a large extent the tetrahedral structure of water in a manner similar to that obtainable applying pressure to a sample of pure water. In particular, the hydrogen site of trigonelline carboxyl group is involved in strong hydrogen bond with the solvent, contributing to a total of about 4 water molecules hydrogen bonded to each trigonelline molecules. Furthermore, trigonelline clustering, not mediated by water, is found in the simulation box. The investigated solution is made up not only by water and trigonelline (both as a positively charged and a zwitterionic species), but it also includes a number of hydronium ions along with chloride ions dissociated from the nitrogen site of each trigonelline molecule. The presence of hydronium ions in solution results in observable Zundel-like com-

plexes, while the chloride ion environment is mostly made up by water molecules.

### CRedit authorship contribution statement

**Michael Di Gioacchino:** Writing – review & editing, Validation, Software, Methodology, Formal analysis, Data curation. **Maria Antonietta Ricci:** Writing – review & editing, Methodology, Investigation. **Fabio Bruni:** Writing – review & editing, Writing – original draft, Visualization, Supervision, Resources, Methodology, Investigation, Conceptualization.

### Declaration of competing interest

The authors declare that they have no known competing financial interests or personal relationships that could have appeared to influence the work reported in this paper.

### Data availability

Data will be made available on request.

### Acknowledgements

The authors wish to acknowledge the contribution of Dr. Emanuele Giordano. The Grant of Excellence Departments 2023–2027, MIUR (ARTICOLO 1, COMMI 314–337 LEGGE 232/2016) is gratefully acknowledged by the authors. Experiment has been performed at the ISIS Neutron and Muon source, supported by beamtime allocation from Science and Technology Facilities Council under the RB number 1710022 available [here](#). This work was performed within the agreement No. 0018318 (06/10/2021) between STFC and CNR, concerning collaboration on scientific research done at ISIS and with partial financial support by CNR.

### References

- [1] E. Illy, A. Illy, The science of a perfect cup of coffee, *Sci. Am.*, <https://www.scientificamerican.com/article/the-science-of-a-perfect-cup-of-coffee/>, 2015.
- [2] A.J. Taylor, D.S. Mottram, *Flavour Science: Recent Developments*, vol. 197, Royal Society of Chemistry, 1996.
- [3] G. Caprioli, et al., Quantification of caffeine, trigonelline and nicotinic acid in espresso coffee: the influence of espresso machines and coffee cultivars, *Int. J. Food Sci. Nutr.* 65 (2014) 465.
- [4] A. Illy, R. Viani, *Espresso Coffee: The Science of Quality*, Academic Press, 2014.
- [5] D. Perrone, C.M. Donangelo, A. Farah, Fast simultaneous analysis of caffeine, trigonelline, nicotinic acid and sucrose in coffee by liquid chromatography-mass spectrometry, *Food Chem.* 110 (2008) 1030.
- [6] D. do Carmo Carvalho, et al., Organic and Conventional Coffea arabica L.: a comparative study of the chemical composition and physiological, biochemical and toxicological effects in Wistar rats, *Plant Foods Hum. Nutr.* 66 (2011) 114.
- [7] N.P. Rodrigues, T.d.J.G. Salva, N. Bragagnolo, Influence of coffee genotype on bioactive compounds and the in vitro capacity to scavenge reactive oxygen and nitrogen species, *J. Agric. Food Chem.* 63 (2015) 4815.
- [8] M. Florin, E.H. Stotz, *Comprehensive Biochemistry*, Elsevier, 1965.
- [9] T.A. Henry, *The Plant Alkaloids*, Forgotten Books, 2018.
- [10] J. Cannon, et al., Isolation, crystal structure and synthesis of arsenobetaine, a constituent of the western rock lobster, the dusky shark, and some samples of human urine, *Aust. J. Chem.* 34 (1981) 787.
- [11] M. Szafran, J. Koput, Z. Dega-Szafran, M. Pankowski, Ab initio and DFT calculations of the structure and vibrational spectra of trigonelline, *J. Mol. Struct.* 614 (2002) 97.
- [12] J. Zhou, L. Chan, S. Zhou, Trigonelline: a plant alkaloid with therapeutic potential for diabetes and central nervous system disease, *Curr. Med. Chem.* 19 (2012) 3523.
- [13] I. Banik, M.N. Roy, Structural effects of three carbohydrates in nicotinic acid/water mixed solvents, *J. Mol. Liq.* 203 (2015) 66.
- [14] M. Di Gioacchino, F. Bruni, S. Imberti, M.A. Ricci, Hydration of carboxyl groups: a route toward molecular recognition?, *J. Phys. Chem. B* 124 (2020) 4358.
- [15] M. Colonna-Dashwood, C.H. Hendon, *Water for Coffee*, Independent Publishing Network, 2015.
- [16] C.H. Hendon, *Chemistry and Coffee*, Matter 2 (2020) 514.
- [17] A.K. Soper, W.S. Howells, A.C. Hannon, ATLAS – analysis of time-of-flight diffraction data from liquid and amorphous samples (RAL–89-046), 1989.
- [18] A.K. Soper, Empirical potential Monte Carlo simulation of fluid structure, *Chem. Phys.* 202 (1996) 295.
- [19] A.K. Soper, Partial structure factors from disordered materials diffraction data: an approach using empirical potential structure refinement, *Phys. Rev. B* 72 (2005) 104204.
- [20] A.K. Soper, GudrunN and GudrunX: programs for correcting raw neutron and X-ray diffraction data to differential scattering cross section (RAL-TR-2011-013), 2011.
- [21] V.F. Sears, Neutron scattering lengths and cross sections, *Neutron News* 3 (1992) 26.
- [22] S.E. Pagnotta, S.E. McLain, A.K. Soper, F. Bruni, M.A. Ricci, Water and trehalose: how much do they interact with each other?, *J. Phys. Chem. B* 114 (2010) 4904.
- [23] E. Scoppola, A. Sodo, S.E. McLain, M.A. Ricci, F. Bruni, Water-peptide site-specific interactions: a structural study on the hydration of glutathione, *Biophys. J.* 106 (2014) 1701.
- [24] L. Tavagnacco, et al., Hydration of caffeine at high temperature by neutron scattering and simulation studies, *J. Phys. Chem. B* 119 (2015) 13294.
- [25] L. Maugeri, et al., Structure-activity relationships in carbohydrates revealed by their hydration, *Biochim. Biophys. Acta G, Gen. Subj.* 1861 (2017) 1486.
- [26] N.H. Rhys, F. Bruni, S. Imberti, S.E. McLain, M.A. Ricci, Glucose and mannose: a link between hydration and sweetness, *J. Phys. Chem. B* 121 (2017) 7771.
- [27] F. Bruni, et al., Hydrogen bond length as a key to understanding sweetness, *J. Phys. Chem. Lett.* 9 (2018) 3667.
- [28] A.K. Soper, M.A. Ricci, F. Bruni, N.H. Rhys, S.E. McLain, Trehalose in water revisited, *J. Phys. Chem. B* 122 (2018) 7365.
- [29] M. Di Gioacchino, F. Bruni, A. Sodo, S. Imberti, M.A. Ricci, Ectoine hydration, aggregation and influence on water structure, *Mol. Phys.* 117 (2019) 3311.
- [30] M. Di Gioacchino, F. Bruni, M.A. Ricci, N-methylacetamide aqueous solutions: a neutron diffraction study, *J. Phys. Chem. B* 123 (2019) 1808.
- [31] M. Di Gioacchino, M.A. Ricci, S. Imberti, N. Holzmann, F. Bruni, Hydration and aggregation of a simple amino acid: the case of glycine, *J. Mol. Liq.* 301 (2020) 112407.
- [32] M. Di Gioacchino, F. Bruni, M.A. Ricci, Hydration of two artificial sweeteners: possible relevance for their taste, *J. Mol. Liq.* 320 (2020) 114398.
- [33] M. Di Gioacchino, F. Bruni, M.A. Ricci, Aqueous solution of betaine: hydration and aggregation, *J. Mol. Liq.* 318 (2020) 114253.
- [34] M. Di Gioacchino, F. Bruni, M.A. Ricci, GPG-NH<sub>2</sub> solutions: a model system for  $\beta$ -turns formation. Possible role of trehalose against drought, *J. Mol. Liq.* 335 (2021) 116514.
- [35] M. Di Gioacchino, F. Bruni, O.L.G. Alderman, M.A. Ricci, Interaction of trehalose and glucose with a peptide  $\beta$ -turn in aqueous solution, *J. Mol. Liq.* 349 (2022) 118451.
- [36] W.L.J. Jorgensen, D.S. Maxwell, J. Tirado-Rives, Development and testing of the OPLS all-atom force field on conformational energetics and properties of organic liquids, *J. Am. Chem. Soc.* 118 (1996) 11225.
- [37] H.J.C. Berendsen, J.R. Grigera, T.P. Straatsma, The missing term in effective pair potentials, *J. Phys. Chem.* 91 (1987) 6269.
- [38] I.M. Svishchev, A.Yu Zassetsky, P.G. Kusalik, Solvation structures in three dimensions, *Chem. Phys.* 258 (2000) 181.
- [39] A.K. Soper, The radial distribution functions of water as derived from radiation total scattering experiments: is there anything we can say for sure?, *ISRN Phys. Chem.* 2013 (2013) 1.
- [40] R. Mancinelli, A. Botti, F. Bruni, M.A. Ricci, A.K. Soper, Perturbation of water structure due to monovalent ions in solution, *Phys. Chem. Chem. Phys.* 9 (2007) 2959.
- [41] R. Mancinelli, A. Botti, F. Bruni, M.A. Ricci, A.K. Soper, Hydration of sodium, potassium, and chloride ions in solution and the concept of structure maker/breaker, *J. Phys. Chem. B* 111 (2007) 13570.
- [42] A. Botti, F. Bruni, S. Imberti, M.A. Ricci, A.K. Soper, Ions in water: the microscopic structure of concentrated NaOH solutions, *J. Chem. Phys.* 120 (2004) 10154.
- [43] C. Zhang, S. Yue, A.Z. Panagiotopoulos, et al., Dissolving salt is not equivalent to applying a pressure on water, *Nat. Commun.* 13 (2022) 822.
- [44] A.K. Soper, The structure of water and aqueous systems, *Exp. Methods Phys. Sci.* 49 (2017) 135.
- [45] A.K. Soper, F. Bruni, M.A. Ricci, Water confined in Vycor glass. II. Excluded volume effects on the radial distribution functions, *J. Chem. Phys.* 109 (1998) 1486.
- [46] A. Botti, F. Bruni, M.A. Ricci, A.K. Soper, Eigen versus Zundel complexes in HCl-water mixtures, *J. Chem. Phys.* 125 (2006) 014508.
- [47] D. Marx, M.E. Tuckerman, J. Hutter, M. Parrinello, The nature of the hydrated excess proton in water, *Nature* 397 (1999) 601.
- [48] P.B. Calio, C. Li, G.A. Voth, Resolving the structural debate for the hydrated excess proton in water, *J. Am. Chem. Soc.* 143 (2021) 18672.
- [49] T. Yamaguchi, N. Fukuyama, K. Yoshida, Y. Katayama, Ion solvation and water structure in an aqueous sodium chloride solution in the gigapascal pressure range, *J. Phys. Chem. Lett.* 12 (2021) 250.
- [50] I. Waluyo, D. Nordlund, U. Bergmann, D. Schlesinger, L.G.M. Pettersson, A. Nilsson, A different view of structure-making and structure-breaking in alkali halide aqueous solutions through x-ray absorption spectroscopy, *J. Chem. Phys.* 140 (2014) 244506.
- [51] J.L. Fulton, M. Balasubramanian, Structure of hydronium (H<sub>3</sub>O<sup>+</sup>)/chloride (Cl<sup>-</sup>) contact ion pairs in aqueous hydrochloric acid solution: a Zundel-like local configuration, *J. Am. Chem. Soc.* 132 (2010) 12597.
- [52] B. Hribar, N.T. Southall, V. Vlachy, K.A. Dill, How ions affect the structure of water, *J. Am. Chem. Soc.* 124 (2002) 12302.



- [53] A. Botti, F. Bruni, S. Imberti, M.A. Ricci, A.K. Soper, Ions in water: the microscopic structure of a concentrated HCl solution, *J. Chem. Phys.* 121 (2004) 7840.
- [54] W. Kunz, P. Lo Nostro, B.W. Ninham, The present state of affairs with Hofmeister effects, *Curr. Opin. Colloid Interface Sci.* 9 (2004) 1.
- [55] Y. Zhang, P.S. Cremer, Interactions between macromolecules and ions: the Hofmeister series, *Curr. Opin. Chem. Biol.* 10 (2006) 658.
- [56] T. Corridoni, R. Mancinelli, M.A. Ricci, F. Bruni, Viscosity of aqueous solutions and local microscopic structure, *J. Phys. Chem. B* 115 (2011) 14008.